Inorg. Chem. **2004**, *43*, 3200–3209

Dendrimers with a Copper(I) Bis(phenanthroline) Core: Synthesis, Electronic Properties, and Kinetics

Elzbieta Gumienna-Kontecka,[†] Yannick Rio,[‡,§] Cyril Bourgogne,[‡] Mourad Elhabiri,[†] Rémy Louis,[||] Anne-Marie Albrecht-Gary,*[,†] and Jean-François Nierengarten*[,§]

Laboratoire de Physico-Chimie Bioinorganique, Université Louis Pasteur et CNRS (UMR 7509), Ecole Européenne de Chimie, Polymères et Matériaux (ECPM), 25 rue Becquerel, 67087 Strasbourg Cedex 2, France, Groupe des Matériaux Organiques, Institut de Physique et Chimie des Matériaux de Strasbourg, Université Louis Pasteur et CNRS (UMR 7504), 23 rue du Loess, B.P. 43, 67034 Strasbourg, France, Groupe de Chimie des Fullerènes et des Systèmes Conjugués, Université Louis Pasteur et CNRS (UMR 7504), ECPM, 25 rue Becquerel, 67087 Strasbourg Cedex 2, France, and Laboratoire d'Electrochimie et de Chimie Physique du Corps Solide, Université Louis Pasteur et CNRS (UMR 7512), 4 rue Blaise Pascal, 67070 Strasbourg Cedex, France

Received January 13, 2004

The copper(I) bis(chelate) complex **Cu(L^0)$_2$** has been prepared from 2,9-diphenethyl-1,10-phenanthroline and $Cu(CH_3CN)_4BF_4$. Derivative **Cu(L^0)$_2$** has been characterized by NMR, UV–vis spectroscopy, and X-ray crystallography. Interestingly, owing to the presence of the ethylene linker, the interligand π–π stacking interactions between the phenyl rings and the phenanthroline subunits in **Cu(L^0)$_2$** do not induce significant distortions of the pseudotetrahedral symmetry around the Cu(I) center in the solid state or in solution. Following the synthesis of **Cu(L^0)$_2$**, dendrimers **Cu(L$^{1-4}$)$_2$** with a Cu(I) bis(2,9-diphenethyl-1,10-phenanthroline) core surrounded by Fréchet type dendritic branches have been prepared and the kinetics of their cyanide-assisted demetalation studied. Importantly, the surrounding dendritic wedges have no significant influence on the coordination geometry of the Cu(I) center, as deduced from their absorption spectra. Therefore, the variations of the rate constants only reflect changes resulting from the presence of the dendritic branches. The kinetics of the cyanide-mediated demetalation reaction indeed revealed that cyanide diffusion through the dendritic shell is slightly influenced by the size of the branches. Significant effects were observed in the kinetics when going from the third to the fourth generation and have been ascribed to changes in the lipophilicity around the metallic core as a result of dendritic encapsulation.

Introduction

In recent years, the rapid advances in dendrimer synthetic chemistry have moved toward the creation of functional systems with increased attention to potential applications.[1] This has given impetus to make dendrimer research a truly interdisciplinary branch of science located at the interfaces between chemistry, physics, and biology. Dendritic macromolecules have shown a wide range of physical and chemical properties that make them attractive for applications in fields including drug delivery,[2] catalysis,[3] and optoelectronics.[4] Many future developments will rely on our ability to

* Authors to whom correspondence should be addressed. E-mail: amalbre@chimie.u-strasbg.fr (A.-M.A.-G.); jfnierengarten@chimie.u-strasbg.fr (J.-F.N.).

† Laboratoire de Physico-Chimie Bioinorganique, Université Louis Pasteur et CNRS.

‡ Groupe des Matériaux Organiques, Institut de Physique et Chimie des Matériaux de Strasbourg, Université Louis Pasteur et CNRS.

§ Groupe de Chimie des Fullerènes et des Systèmes Conjugués, ECPM.

|| Laboratoire d'Electrochimie et de Chimie Physique du Corps Solide, Université Louis Pasteur et CNRS.

(1) (a) Newkome, G. R.; Moorefield, C. N.; Vögtle, F. *Dendrimers and Dendrons: Concepts, Syntheses, Applications*; VCH: Weinheim, Germany, 2001. (b) *Dendrimers and other Dendritic Polymers*; Fréchet, J. M. J., Tomalia, D. A., Eds.; Wiley: Chichester, U.K., 2001.

(2) For examples, see: (a) Kono, K.; Liu, M.; Fréchet, J. M. J. *Bioconjugate Chem.* **1999**, *10*, 1115. (b) Malik, N.; Wimattanapatapee, R.; Klopsch, R.; Lorenz, K.; Frey, H.; Weener, J. W.; Meijer, E. W.; Paulus, W.; Duncan, R. *J. Controlled Release* **2000**, *65*, 133. (c) Grinstaff, M. W. *Chem.—Eur. J.* **2002**, *8*, 2839.

(3) (a) Oosterom, G. E.; Reek, J. N. H.; Kamer, P. C. J.; van Leeuwen, P. W. N. M. *Angew. Chem., Int. Ed.* **2001**, *40*, 1828. (b) Twyman, L. J.; King, A. S. H.; Martin, I. K. *Chem. Soc. Rev.* **2002**, *31*, 69. (c) Che, C.-M.; Huang, J.-S.; Zhang, J.-L. *C. R. Chimie* **2003**, *6*, 1105. (d) van Klink, G. P. M.; Dijkstra, H. P.; van Koten, G. *C. R. Chimie* **2003**, *6*, 1079. (e) Ribourdouille, Y.; Engel, G. D.; Gade, L. H. *C. R. Chimie* **2003**, *6*, 1087. (f) Soai, K.; Sato, I. *C. R. Chimie* **2003**, *6*, 1097.

10.1021/ic049945y CCC: $27.50 © 2004 American Chemical Society
Published on Web 04/02/2004

understand their intimate properties. However, structural information is quite difficult to obtain for dendritic molecules. Actually, even if dendrimers have precise compositional and constitutional aspects, they exhibit many possible conformations.[1] In addition, they generally lack long-range order in the condensed phase and structural characterization of large dendrimers by X-ray crystallography is nearly impossible. Therefore, the best way to characterize dendritic structures relies on indirect spectroscopic methods.[5] As part of this research, the systematic study of dendrimers with an active core unit as a function of the generation number is of particular interest.[5,6] Information about the shielding of the central unit is derived from the effect the dendritic shell has on some specific properties of the core. For example, kinetic studies of chemical reactions involving the central core unit give insight into substrate diffusion through the dendritic shell and allow for an evaluation of the accessibility of the core.[5] On the other hand, specific changes in the microenvironment of electroactive[7] and/or photoactive[5,8] cores are conveniently analyzed by monitoring the redox and/or photophysical properties as a function of the generation number. In a recent paper,[9] we reported the synthesis and the electrochemical properties of the dendritic Cu(I) bis(phenanthroline) complexes derived from ligands $\mathbf{L^{0-4}}$ (Scheme 1). When the size of the dendritic shell is increased, the electron transfer kinetics are attenuated. This effect has been observed for several examples of dendrimers with an electroactive core[7] and illustrates the dendritic shell effect that leads to a more hindered approach of the core to the electrode.

In this paper, we now report in detail the preparation of $\mathbf{L^{0-4}}$ and of the corresponding Cu(I) complexes $\mathbf{Cu(L^{0-4})_2}$. The X-ray structure of $\mathbf{Cu(L^0)_2}$ in the solid state has been resolved. In solution, NMR and UV−vis characterization and cyanide-assisted dissociation kinetics of the $\mathbf{L^{0-4}}$ bis(chelate)-cuprous complexes have been carried out. For the sake of comparison, the demetalation kinetics of the Cu(I) complexes of neocuproine (2,9-dimethyl-1,10-phenanthroline = dmp) and 2,9-di(*p*-anisyl)-1,10-phenanthroline (dap) have been also examined.

Scheme 1

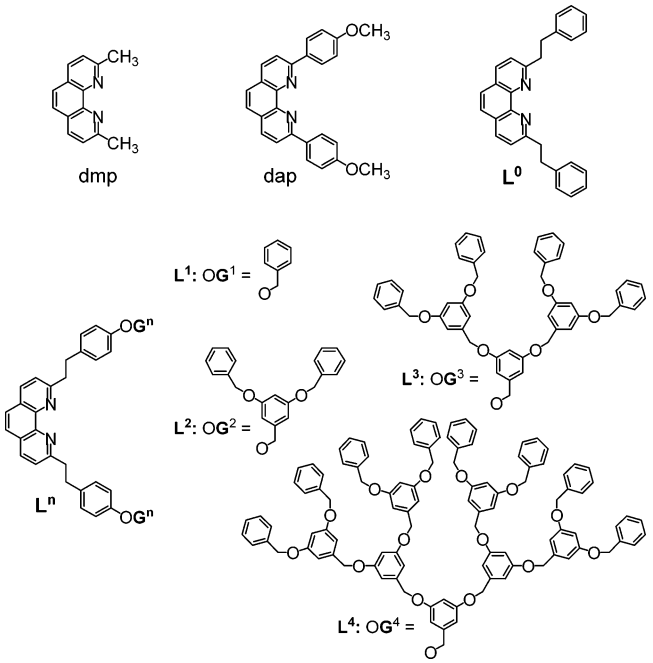

Scheme 2. Preparation of $\mathbf{Cu(L^0)_2}$[a]

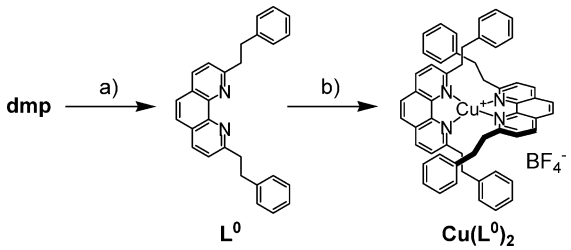

[a] Reagents and conditions: (a) LDA (2 equiv), THF, −78 °C, then benzyl bromide, −78 °C to room temp (55%); (b) $Cu(CH_3CN)_4BF_4$, CH_2Cl_2, CH_3CN, room temp (96%).

Results and Discussion

Synthesis and X-ray Crystal Structure of $\mathbf{Cu(L^0)_2}$. The synthesis of the Cu(I) complex $\mathbf{Cu(L^0)_2}$ is depicted in Scheme 2. Compound $\mathbf{L^0}$ was prepared from dmp by deprotonation of the methyl groups with lithium diisopropylamide (LDA) to generate the corresponding dicarbanionic species,[10] followed by reaction with benzyl bromide. The Cu(I) complex $\mathbf{Cu(L^0)_2}$ was then obtained in 96% yield by treatment of $\mathbf{L^0}$ with $Cu(CH_3CN)_4BF_4$ in CH_2Cl_2/CH_3CN at room temperature.

The air-stable complex $\mathbf{Cu(L^0)_2}$ was characterized by ^1H and ^{13}C NMR spectroscopy, elemental analysis, and X-ray crystallography. In the structure, two different conformers (noted **A** and **B**) are observed for the $\mathbf{Cu^+(L^0)_2}$ cation. As shown in Figure 1, the main difference among them is the orientation of the four terminal phenyl subunits. In the first one, the two phenyl groups of both ligands are located on either side of the plane of their phenanthroline core (*anti* conformation) and cation **A** adopts a helical type structure. In contrast, whereas one ligand of cation **B** is also in an *anti* conformation, the two phenyl moieties belonging to the other

(4) (a) Balzani, V.; Campagna, S.; Denti, G.; Juris, A.; Serroni, S.; Venturi, M. *Acc. Chem. Res*. **1998**, *31*, 26. (b) Fisher, M.; Vögtle, F. *Angew. Chem., Int. Ed.* **1999**, *38*, 884. (c) Adronov, A.; Fréchet, J. M. J. *Chem. Commun*. **2000**, 1701. (d) Balzani, V.; Ceroni, P.; Juris, A.; Venturi, M.; Campagna, S.; Puntoriero, F.; Serroni, S. *Coord. Chem. Rev.* **2001**, *219*, 545. (e) Newkome, G. R.; He, E.; Moorefield, C. N. *Chem. Rev.* **1999**, *99*, 1689. (f) Berresheim, A. J.; Müller, M.; Müllen, K. *Chem. Rev*. **1999**, *99*, 1747. (g) Zeng, F.; Zimmerman, S. C. *Chem. Rev.* **1997**, *97*, 1681. (h) Chow, H.-F.; Mong, T. K.-K.; Nongrum, M. F.; Wan, C.-W. *Tetrahedron* **1998**, *54*, 8543. (i) Smith, D. K.; Diederich, F. *Chem.—Eur. J*. **1998**, *4*, 1353. (j) Bosman, A. W.; Janssen, H. M.; Meijer, E. W. *Chem. Rev*. **1999**, *99*, 1665. (k) Adronov, A.; Fréchet, J. M. J. *Chem. Commun.* **2000**, 1701. (l) Inoue, K. *Prog. Polym. Sci.* **2000**, *25*, 453. (m) Nierengarten, J.-F. *Top. Curr. Chem.* **2003**, *228*, 87.
(5) (a) Hecht, S.; Fréchet, J. M. J. *Angew. Chem., Int. Ed.* **2001**, *40*, 74 and references therein. (b) Gorman, C. B.; Smith, J. C. *Acc. Chem. Res.* **2001**, *34*, 60.
(6) Nierengarten, J.-F. *C. R. Chimie* **2003**, *6*, 725.
(7) (a) Cameron, C. S.; Gorman, C. B. *Adv. Funct. Mater*. **2002**, *12*, 17 and references therein. (b) Gorman, C. B. *C. R. Chimie* **2003**, *6*, 911.
(8) Nierengarten, J.-F.; Armaroli, N.; Accorsi, G.; Rio, Y.; Eckert, J.-F. *Chem.—Eur. J*. **2003**, *9*, 36.
(9) Rio, Y.; Accorsi, G.; Armaroli, N.; Felder, D.; Levillain, E.; Nierengarten, J.-F. *Chem. Commun.* **2002**, 2830.
(10) Nierengarten, J.-F.; Dietrich-Buchecker, C. O.; Sauvage, J.-P. *New J. Chem.* **1996**, *20*, 685.

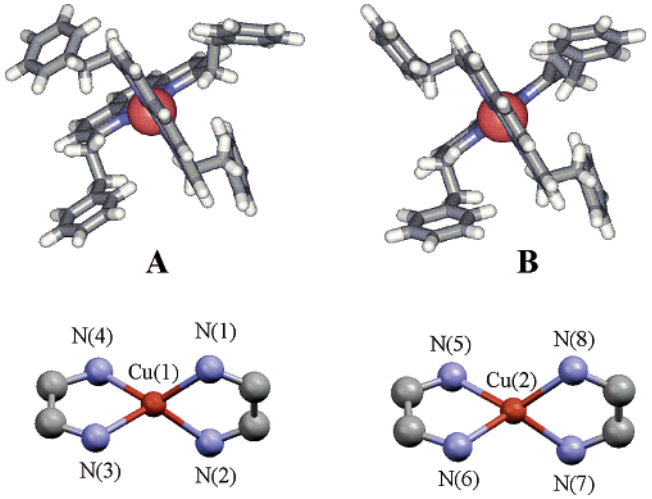

Figure 1. Representation of the two conformers of $\mathbf{Cu^{+}(L^{0})_2}$ seen in the X-ray crystal structure and details of the coordination sphere around the Cu(I) cation for both of them.

Table 1. Bond Distances (Å) and Angles (deg) within the Coordination Spheres for Both Conformers of $\mathbf{Cu(L^{0})_2}$ (See Figure 1 for the Numbering)

conformer **A**		conformer **B**	
Cu(1)−N(1)	2.020(9)	Cu(2)−N(5)	2.029(7)
Cu(1)−N(2)	2.023(9)	Cu(2)−N(6)	2.041(8)
Cu(1)−N(3)	2.027(8)	Cu(2)−N(7)	2.024(8)
Cu(1)−N(4)	2.027(8)	Cu(2)−N(8)	2.047(8)
N(1)−Cu(1)−N(2)	83.4(4)	N(5)−Cu(2)−N(6)	82.3(3)
N(1)−Cu(1)−N(3)	126.4(3)	N(5)−Cu(2)−N(7)	128.5(3)
N(1)−Cu(1)−N(4)	124.7(3)	N(5)−Cu(2)−N(8)	123.4(4)
N(2)−Cu(1)−N(3)	122.6(3)	N(6)−Cu(2)−N(7)	121.6(3)
N(2)−Cu(1)−N(4)	122.6(4)	N(6)−Cu(2)−N(8)	124.8(3)
N(3)−Cu(1)−N(4)	82.6(4)	N(7)−Cu(2)−N(8)	82.2(3)

one are located on the same side relative to the plane of their phenanthroline unit (*syn* conformation).

The coordination sphere around the Cu(I) cation is quite similar for both conformers (Figure 1 and Table 1). In crude terms, the coordination geometry is pseudotetrahedral, but there are some significant deviations from the tetrahedral symmetry. In particular, the chelate-bite angle is only 82.2−83.4°, a typical value for such phenanthroline complexes.[11−14] However, unlike what is typically seen in the solid state structures of related copper(I) complexes, there is no flattening of the two ligands relative to one another (toward a square-planar geometry) as a consequence of the crystal packing forces.[11−14] Effectively, the dihedral angle between the ligands planes is almost 90° for both **A** and **B**. As a consequence, the four Cu−N distances are almost identical and the geometry of the copper/nitrogen framework is quite regular by comparison with the cases of other Cu(I) bis-(phenanthroline) complexes.

In addition to several intramolecular face-to-edge π stacking interactions between the phenanthroline moiety of one ligand and the phenyl subunits of the other one in both **A** and **B**, close inspection of the crystal packing reveals a network of intermolecular π stacking interactions between the different aromatic rings of neighboring $\mathbf{Cu^{+}(L^{0})_2}$ cations. For example, the simultaneous $\pi-\pi$ interactions of a phenyl unit of cation **A** with two aromatic rings of the neighboring cation **B** are highlighted in Figure 2A. Specifically, a phenanthroline moiety and a phenyl ring belonging to the second ligand of cation **B** are both involved in intermolecular $\pi-\pi$ stacking interactions with the same phenyl unit of **A**. It can be added that the two aromatic rings of **B** giving rise to this intermolecular stacking are themselves in $\pi-\pi$ interactions in a face-to-edge manner. As previously mentioned, there is no flattening of the two ligands relative to one another due to the crystal packing forces. It seems that the latest forces have only an influence on the dihedral angle between the phenanthroline core and the terminal phenyl subunits. In other words, rotation around the CH_2CH_2 linker is sufficient to optimize intermolecular contacts within the crystal lattice and there is no need to further distort the coordination sphere around the Cu(I) cation.

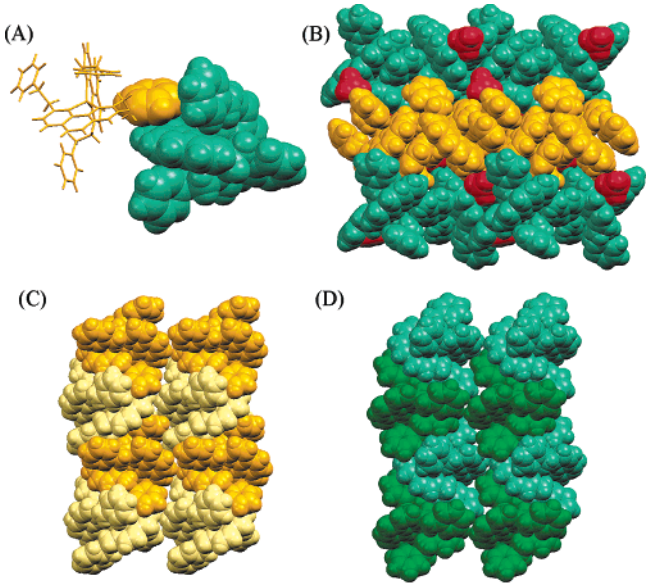

Figure 2. Stacking within the $\mathbf{Cu(L^{0})_2}$ lattice. (A) View highlighting intermolecular $\pi-\pi$ stacking interactions between two neighboring cations (orange, conformer **A**; green, conformer **B**). (B) View down the crystallographic axis *a* revealing alternated layers of the two conformers of the $\mathbf{Cu^{+}(L^{0})_2}$ cation in the X-ray crystal structure (orange, conformer **A**; green, conformer **B**; red, the BF_4^- anions). (C) Details of the packing in the layer containing conformer **A** (view down the crystallographic axis *c*). (D) Details of the packing in the layer containing conformer **B** (view down the crystallographic axis *c*).

Observation of the crystal lattice down the crystallographic axis *a* reveals alternated layers of cations **A** and **B** (Figure 2B). Within the layer formed by conformer **A**, the $\mathbf{Cu^{+}(L^{0})_2}$ cations are organized in columnar arrays parallel to the crystallographic axis *b* (Figure 2C). As already mentioned, cation **A** adopts a helical type structure, and it can be noted that the columns alternate right- and left-handed helical conformers. As shown in Figure 2D, a similar organization is observed within the layer containing the $\mathbf{Cu^{+}(L^{0})_2}$ cation **B**.

(11) Eggleston, M. K.; Fanwick, P. E.; Pallenberg, A. J.; McMillin, D. R. *Inorg. Chem.* **1997**, *36*, 4007.
(12) Klemens, F. K.; Palmer, C. E. A.; Rolland, S. M.; Fanwick, P. E.; McMillin, D. R.; Sauvage, J.-P. *New J. Chem.* **1990**, *14*, 129.
(13) Dobson, J. F.; Green, B. E.; Healy, P. C.; Kennard, C. H. L.; Pakawatchai, C.; White, A. H. *Aust. J. Chem.* **1984**, *37*, 649.
(14) Klemens, F. K.; Fanwick, P. E.; Bibler, P. E.; McMillin, D. R. *Inorg. Chem.* **1989**, *28*, 3076.

Scheme 3. Preparation of $\mathbf{Cu(L^{1-4})_2}$[a]

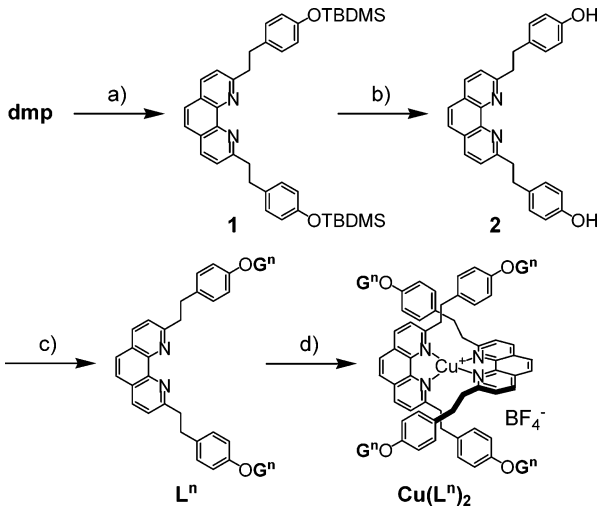

[a] Reagents and conditions: (a) LDA (2 equiv), THF, −78 °C, then *p*-[(*tert*-butyldimethylsilyl)oxy]benzyl bromide, −78 °C to room temp (38%); (b) TBAF, THF, 0 °C (97%); (c) $\mathbf{G^nBr}$, K_2CO_3, 18-C-6, acetone, Δ ($n = 1$, 76%; $n = 2$, 95%; $n = 3$, 96%; $n = 4$, 99%); (d) $Cu(CH_3CN)_4BF_4$, CH_2Cl_2, CH_3CN, room temp ($n = 1$, 95%; $n = 2$, 72%; $n = 3$, 92%; $n = 4$, 85%).

Synthesis and Characterization of the Dendritic Cu(I) Complexes $\mathbf{Cu(L^{1-4})_2}$. The synthesis of the dendritic ligands $\mathbf{L^{1-4}}$ and the corresponding Cu(I) complexes is shown in Scheme 3. Treatment of dmp with LDA at −78 °C followed by reaction of the resulting dicarbanion with *p*-[(*tert*-butyldimethylsilyl)oxy]benzyl bromide gave **1** in a moderate yield (38%). Actually, products of monoalkylation were also formed in the reaction, making the purification of **1** particularly difficult. However, since sufficient quantities of compound **1** were thus obtained, no particular efforts were made to optimize this step. Cleavage of the phenolic TBDMS ethers in **1** was then achieved by reaction with an excess of tetrabutylammonium fluoride (TBAF) in THF at 0 °C. Diphenol **2** thus obtained was treated with benzyl bromide $\mathbf{G^1Br}$ in the presence of K_2CO_3 and 18-crown-6 (18-C-6) in refluxing acetone to give the first generation ligand $\mathbf{L^1}$. The next generation compounds $\mathbf{L^{2-4}}$ were prepared by reaction of **2** with the corresponding Fréchet type dendritic benzylic bromides[15] $\mathbf{G^{2-4}Br}$ under similar conditions. The dendritic Cu(I) complexes $\mathbf{Cu(L^{1-4})_2}$ were finally obtained in good yields by treatment of the corresponding ligands $\mathbf{L^{1-4}}$ with $Cu(CH_3CN)_4BF_4$ in CH_2Cl_2/CH_3CN at room temperature. The coordination of the phenanthroline ligand to the Cu(I) cation was easily observed by an instantaneous color change of the solution upon addition of the Cu(I) salt. Actually, the colorless ligand solution became orange-red due to the apparition of the metal-to-ligand charge transfer (MLCT) band characteristic of the Cu(I) bis(2,9-disubstituted-1,10-phenanthroline) derivatives (see below). Compounds $\mathbf{Cu(L^{1-4})_2}$ were characterized by ^1H and ^{13}C NMR spectroscopy and elemental analysis. In addition, the structures of dendrimers $\mathbf{Cu(L^{2-4})_2}$ were also confirmed by MALDI-TOF mass spectrometry, with no peaks corresponding to defected dendrimers being observed. In all the cases, a singly charged ion peak assigned to the Cu(I) complex after loss of the tetrafluoroborate counteranion ($[M - BF_4]^+$) was observed.

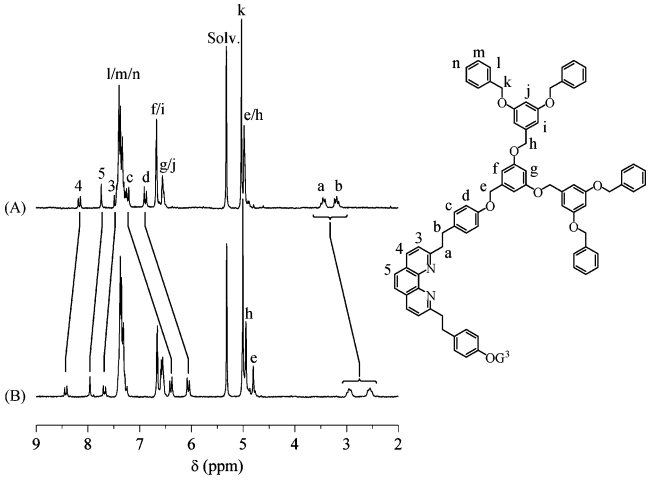

Figure 3. ^1H NMR spectra (200 MHz, CD_2Cl_2, 25 °C) of (A) $\mathbf{L^3}$ and (B) $\mathbf{Cu(L^3)_2}$.

The ^1H NMR spectra of $\mathbf{Cu(L^{1-4})_2}$ provided good evidence for their formation. Effectively, as a result of the ring current effect of one phenanthroline subunit on the 2,9-substituents of the second one in the complex, the signals of the protons belonging to the groups directly attached to the phenanthroline core are shielded by about 1.0 ppm in $\mathbf{Cu(L^{1-4})_2}$ when compared to the signals in the corresponding ligands $\mathbf{L^{1-4}}$. This particular behavior is specific of such copper(I) complexes.[16] As a typical example, the ^1H NMR spectra of $\mathbf{L^3}$ and $\mathbf{Cu(L^3)_2}$ recorded in CD_2Cl_2 are shown in Figure 3.

In addition to the signals corresponding to the dendritic branches, the ^1H NMR spectrum of $\mathbf{L^3}$ is characterized by two sets of AB quartets and a singlet in a typical pattern for a 2,9-disubstituted-1,10-phenanthroline: an AA′XX′ system for the *p*-disubstituted phenyl ring and an A_2X_2 system for the CH_2CH_2 linker. Upon complexation to the Cu(I) cation, dramatic changes are observed for the chemical shifts of H_a, H_b, H_c, H_d, and H_e, showing that the CH_2CH_2−phenyl−OCH_2 moieties attached to one phenanthroline ligand are located on either side of the other one in $\mathbf{Cu(L^3)_2}$. In addition, the particularly important shielding observed for the signals of protons H_c and H_d also suggests strong interligand $\pi-\pi$ stacking interactions in the Cu(I) complex between the *p*-disubstituted phenyl rings and the phenanthroline subunits. This appears quite reasonable on the basis of the X-ray crystal structure of the corresponding model compound $\mathbf{Cu(L^0)_2}$. It can also be noted that there are no complexation-induced changes in the chemical shifts for the signals corresponding to the poly(benzyl ether) dendritic wedges. The latter observation suggests that there are no particular π stacking interactions between the phenanthroline moieties and the dendritic benzylic units in CH_2Cl_2 solutions.

Electronic Absorption Spectra. The electronic spectra of $\mathbf{Cu(dmp)_2}$, $\mathbf{Cu(dap)_2}$, and $\mathbf{Cu(L^n)_2}$ were recorded under

(15) (a) Hawker, C.; Fréchet, J. M. J. *Chem. Commun*. **1990**, 1010. (b) Hawker, C.; Fréchet, J. M. J. *J. Am. Chem. Soc.* **1990**, *112*, 7638.

(16) Dietrich-Buchecker, C. O.; Marnot, P. A.; Sauvage, J.-P.; Kintzinger, J.-P. *Nouv. J. Chim.* **1984**, *8*, 573.

Table 2. Absorption Maxima and Extinction Coefficients of **Cu(dmp)$_2$**, **Cu(dap)$_2$**, and **Cu(L^n)$_2$**[a]

	λ_{max} (nm) (ϵ_{max} (M^{-1} cm^{-1}))	
compound	$CH_2Cl_2/CH_3CN/H_2O$ = 50/48/2 (v/v/v)[a]	$CH_2Cl_2/CH_3CN/H_2O$ = 15/80/5 (v/v/v)[b]
Cu(dmp)$_2$	456 (8360)	455 (8300)
Cu(dap)$_2$	430 (2610)	430 (2800)
Cu(L^0)$_2$	455 (6050)	
Cu(L^1)$_2$	455 (5300)	
Cu(L^2)$_2$	456 (6100)	
Cu(L^3)$_2$	456 (6100)	
Cu(L^4)$_2$	456 (6150)	

[a] I = 0.05 M (Bu_4NBF_4); T = 25.0 ± 0.2 °C. [b] I = 0.1 M (n-$C_4H_9)_4NCF_3SO_3$; T = 25.0 ± 0.1 °C; ref 17. The errors were estimated to be within 1 nm for the wavelengths and 5% for the extinction coefficients.

the experimental conditions used for the kinetic studies (see below) and are depicted in Figure 4 and Supporting Information Figure S1. By comparison with the cases of previous studies,[17] the visible absorption of **Cu(dmp)$_2$** and **Cu(dap)$_2$** appears not to be significantly sensitive to changes of ionic strength and solvent (Table 2).

The absorption spectra of **Cu(L^n)$_2$** (350−600 nm) display the characteristic features of Cu(I) bis(phenanthroline) complexes. Their MLCT bands are constituted by a main absorption (band II) centered at 455 nm with two satellite shoulders (bands III and I) at 380 and 510 nm, respectively (Figure 4 and Supporting Information Figure S1). Band II corresponds to the $b_2(xz) \rightarrow b_3(\psi)$ transition polarized along the z axis which joins the metal and ligand centers. The shoulders at lower (band I) and higher (band III) energies have been attributed to the $b_3(yz) \rightarrow b_2(\psi)$ transition polarized along the z axis and to the $b_3(yz) \rightarrow a(\chi)$ and $b_3(yz) \rightarrow b_1(\chi)$ transitions polarized along the x and y axes, respectively.[11,18−21]

Interestingly, the shapes of the MLCT absorption spectra of the dendritic **Cu(L^n)$_2$** complexes are rather similar to that of **Cu(dmp)$_2$**, for which spectral characteristics were assigned assuming a slightly distorted tetrahedral coordination geometry.[18,22−23] In contrast, for **Cu(dap)$_2$**, the tetrahedral symmetry around the copper(I) center is strongly distorted due to the interligand $\pi-\pi$ stacking interactions.[24] This is reflected by a hypochromic blue-shift of the MLCT absorption maximum, bandwidth broadening, and a considerable increase of the absorption of band I relative to that of band II (Figure 4 and Table 2).[11,19] The MLCT absorption features of the **Cu(L^n)$_2$** complexes (Table 2) suggest therefore that

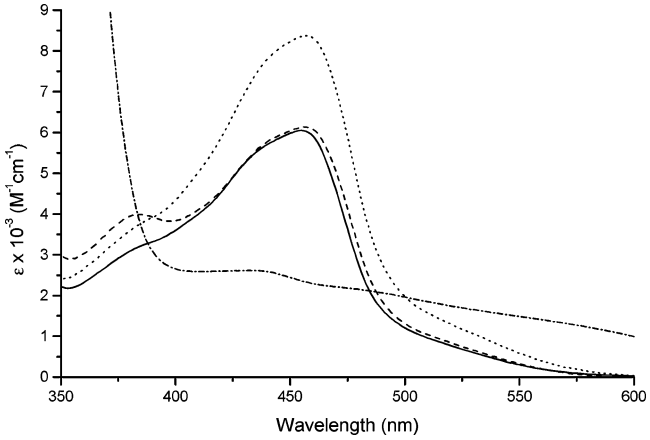

Figure 4. Electronic spectra of the **Cu(dmp)$_2$** (dot), **Cu(dap)$_2$** (dash dot), **Cu(L^0)$_2$** (solid), and **Cu(L^4)$_2$** (dash) complexes. Solvent: $CH_2Cl_2/CH_3CN/H_2O$ = 50/48/2 (v/v/v); I = 0.05 M (Bu_4NBF_4); T = 25.0 ± 0.2 °C.

the interligand $\pi-\pi$ stacking interactions between the phenyl groups and the phenanthroline moieties evidenced by NMR (Figure 3) do not induce significant distortions of the pseudotetrahedral symmetry around the Cu(I) center in solution. The latter observation is in good agreement with the coordination geometry observed for **Cu(L^0)$_2$** in the solid state. Since the spectroscopic properties are not changing within the series of **Cu(L^n)$_2$** complexes (Table 2, Figure 4, and Supporting Information Figure S1), it may be also concluded that increased size of the surrounding dendritic wedges does not affect the electronic structure of the central Cu(I) bis(phenanthroline) core. In other words, the dendrons have no influence on the coordination geometry of the Cu(I) center. This is expected, since the bulky substituents are not directly attached to the phenanthroline ligand.[18]

Kinetics. The cyanide-assisted demetalation of the dendritic Cu(I) complexes **Cu(L^n)$_2$** was studied in an analogous way to that adopted for the Cu(I) catenates.[25] All the experiments were carried out in a freshly prepared homogeneous ternary solvent, $CH_2Cl_2/CH_3CN/H_2O$ = 50/48/2 (v/v/v), which was chosen in order to solubilize both the reactants and the products of the decomplexation reaction. For comparison purposes, the demetalation kinetics of **Cu(dmp)$_2$** and **Cu(dap)$_2$** were also studied under the same experimental conditions. Previous studies on their decomplexation by cyanide were carried out in homogeneous mixed solvents, either CH_3CN/H_2O = 90/10 (by weight)[25] or $CH_2Cl_2/CH_3CN/H_2O$ = 15/80/5 (v/v/v).[26,27] The latter is a suitable solvent for all the **Cu(L^n)$_2$** complexes studied in this work except for the largest one (**Cu(L^4)$_2$**), which demands a higher quantity of CH_2Cl_2. Hence, solvents with an increasing amount of CH_2Cl_2 were tested and the optimal solubility was achieved with a ternary solvent, $CH_2Cl_2/CH_3CN/H_2O$ = 50/48/2 (v/v/v).

(17) Meyer, M.; Albrecht-Gary, A.-M.; Dietrich-Buchecker, C. O.; Sauvage, J.-P. *Inorg. Chem.* **1999**, *38*, 2279.
(18) For a review on the photophysical properties of Cu(I) bis(phenanthroline) derivatives, see: Armaroli, N. *Chem. Soc. Rev.* **2001**, *30*, 113.
(19) Phifer, C. C.; McMillin, D. R. *Inorg. Chem.* **1986**, *25*, 1329.
(20) Parker, W. L.; Crosby, G. A. *J. Phys. Chem.* **1989**, *93*, 5692.
(21) Felder, D.; Nierengarten, J. F.; Barigelletti, F.; Ventura, B.; Armaroli, N. *J. Am. Chem. Soc.* **2001**, *123*, 6291.
(22) Ichinaga, A. K.; Kirchhoff, J. R.; McMillin, D. R.; Dietrich-Buchecker, C. O.; Marnot, P. A.; Sauvage, J.-P. *Inorg. Chem.* **1987**, *26*, 4290.
(23) Everly, R. M.; McMillin, D. R. *J. Phys. Chem.* **1991**, *95*, 9071.
(24) Geoffroy, M.; Wermeille, M.; Dietrich-Buchecker, C. O.; Sauvage, J.-P.; Bernardinelli, J.-P. *Inorg. Chim. Acta* **1990**, *167*, 157.
(25) Albrecht-Gary, A.-M.; Saad, Z.; Dietrich-Buchecker, C. O.; Sauvage, J.-P. *J. Am. Chem. Soc.* **1985**, *107*, 3205.
(26) Chambron, J. C.; Dietrich-Buchecker, C.; Nierengarten, J. F.; Sauvage, J.-P.; Solladié, N.; Albrecht-Gary, A.-M.; Meyer, M. *New J. Chem.* **1995**, *19*, 409.
(27) Meyer, M.; Albrecht-Gary, A.-M.; Dietrich-Buchecker, C. O.; Sauvage, J.-P. *J. Am. Chem. Soc.* **1997**, *119*, 4599.

Table 3. Experimental Pseudo-First-Order Decomplexation Rate Constants of Bis(chelate) Copper(I) Complexes by Cyanide[a]

Cu(dmp)$_2$		**Cu(dap)$_2$**		**Cu(L^0)$_2$**		**Cu(L^1)$_2$**		**Cu(L^2)$_2$**		**Cu(L^3)$_2$**		**Cu(L^4)$_2$**	
$[CN^-]_0$ (mM)	k_{obs} (s^{-1})	$[CN^-]_0$ (mM)	k_{obs} (s^{-1})	$[CN^-]_0$ (mM)	k_{obs} (s^{-1})	$[CN^-]_0$ (mM)	k_{obs} (s^{-1})	$[CN^-]_0$ (mM)	k_{obs} (s^{-1})	$[CN^-]_0$ (mM)	k_{obs} (s^{-1})	$[CN^-]_0$ (mM)	k_{obs} (s^{-1})
0.60	2.44(1)	1.88	0.3348(8)	0.61	0.084(1)	0.60	0.0672(8)	0.59	0.067(2)	0.60	0.0658(8)	0.76	0.068(4)
0.75	3.12(2)	2.82	0.355(4)	0.76	0.114(2)	0.90	0.1172(4)	0.89	0.1154(9)	0.74	0.0900(7)	0.92	0.0907(6)
0.91	3.58(4)	3.27	0.3635(6)	0.92	0.136(1)	1.04	0.1366(9)	1.03	0.1390(7)	0.90	0.1130(7)	1.06	0.108(1)
1.05	4.24(4)	3.76	0.3714(5)	1.06	0.159(1)	1.19	0.1540(7)	1.19	0.1606(5)	1.04	0.1346(9)	1.22	0.128(1)
1.21	4.68(2)	4.25	0.377(1)	1.22	0.183(2)	1.35	0.184(1)	1.34	0.1806(5)	1.20	0.1524(5)	1.36	0.142(1)
1.37	5.22(6)	4.7	0.383(1)	1.36	0.194(1)	1.49	0.204(1)	1.49	0.2068(8)	1.35	0.1734(5)	1.52	0.1603(1)
1.51	5.84(2)	5.64	0.3972(8)	1.52	0.216(1)	1.79	0.244(2)	1.78	0.247(1)	1.49	0.195(1)	1.83	0.1843(6)
1.81	6.88(2)	7.53	0.419(4)	1.83	0.255(1)	2.39	0.3526(5)	2.38	0.346(1)	1.79	0.235(2)	2.44	0.2523(6)
2.12	7.7(1)			2.44	0.344(2)					2.09	0.277(2)		
2.42	8.71(6)									2.39	0.321(2)		

[a] Solvent: $CH_2Cl_2/CH_3CN/H_2O$ = 50/48/2 (v/v/v); I = 0.05 M (Bu_4NBF_4); T = 25.0 ± 0.2 °C. Values in parentheses are errors on the last significant digit estimated as standard deviation, 1σ.

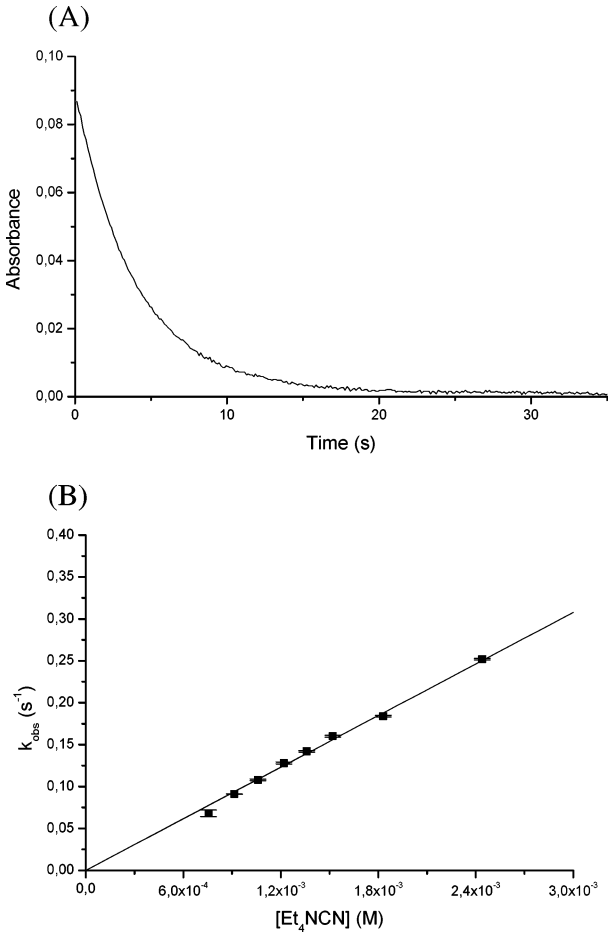

Figure 5. (A) Kinetic trace recorded for the dissociation of complex **Cu(L^4)$_2$** and (B) plot of its pseudo-first-order rate constant, k_{obs}, as a function of cyanide concentration. $[\mathbf{Cu(L^4)_2}]_0 = 1.47 \times 10^{-5}$ M; $[CN^-]_0 = 1.22 \times 10^{-3}$ M. Solvent: $CH_2Cl_2/CH_3CN/H_2O$ = 50/48/2 (v/v/v); I = 0.05 M (Bu_4NBF_4); T = 25.0 ± 0.2 °C; wavelength of detection, λ = 456 nm.

Cyanide anion is a strong nucleophile known to form very stable Cu(I) complexes.[28−30] The cyanide-assisted demetalation kinetics of the bis(chelate) complexes **Cu(dmp)$_2$**, **Cu(dap)$_2$**, and **Cu(L^n)$_2$** have been examined in excess of CN^-. If we suppose that under our experimental conditions the only cuprous product would be $Cu^I(CN)_4^{3-}$, the overall reaction could be written:

$$Cu^I(L)_2^+ + 4CN^- \rightarrow 2L + Cu^I(CN)_4^{3-} \quad (1)$$

A monoexponential absorbance decay observed in the seconds time range indicates a single rate-limiting decomplexation step. The excellent agreement between the initial absorbance and the spectrophotometric data measured for the Cu(I) complexes corresponds to the absence of faster steps prior to the recorded one. As an example, Figure 5A displays the recording of absorption versus time at 465 nm for **Cu(L^4)$_2$**. The variations of the pseudo-first-order rate constants, k_{obs} (Table 3), with the analytical cyanide concentrations show a linear dependence. The corresponding data are given in Figure 5B for the **Cu(L^4)$_2$** complex, while they are presented in Supporting Information Figure S2 for **Cu(dmp)$_2$**, **Cu(dap)$_2$**, and **Cu(L$^{0-3}$)$_2$**.

The second-order rate constants were calculated by nonweighted linear regression and are given together with their corresponding standard deviations[31] in Table 4.

The corresponding rate law is expressed by eq 2, where k_D and k_{CN} (Table 4) stand for the monomolecular dissociation and cyanide-assisted bimolecular rate constants, respectively.

$$v = -\frac{d[Cu^I(L)_2^+]_0}{dt} = k_{obs}[Cu^I(L)_2^+]_0 = \{k_D + k_{CN}[CN^-]_0\}[Cu^I(L)_2^+]_0 \quad (2)$$

Table 4. Kinetic Parameters Relative to the Dissociation of Bis(chelate) Copper(I) Complexes by Cyanide[a]

compound	$k_D \pm \sigma$ (s^{-1})	$k_{CN} \pm \sigma$ (M^{-1} s^{-1})
Cu(dmp)$_2$	0.53 ± 0.09	3423 ± 63
Cu(dap)$_2$	0.314 ± 0.003	14.5 ± 0.8
Cu(L^0)$_2$	*b*	143 ± 2
Cu(L^1)$_2$	*b*	139 ± 3
Cu(L^2)$_2$	*b*	139 ± 3
Cu(L^3)$_2$	*b*	131 ± 2
Cu(L^4)$_2$	*b*	103 ± 1

[a] Solvent: $CH_2Cl_2/CH_3CN/H_2O$ = 50/48/2 (v/v/v); I = 0.05 M (Bu_4NBF_4); T = 25.0 ± 0.2 °C. [b] The value of k_D was constrained to zero.

(28) Kunschert, F. Z. *Z. Anorg. Allg. Chem.* **1904**, *41*, 359.
(29) Bjerrum, J. *Metal Ammine Formation in Aqueous Solution*; P. Haase and Son: Copenhagen, Denmark, 1957.
(30) Hefter, G.; May, P.; Sipos, P. *J. Chem. Soc., Chem. Commun.* **1993**, 1704.
(31) *Microcal Origin*; Microcal Software, Inc.: Northampton, MA, 1991−1997.

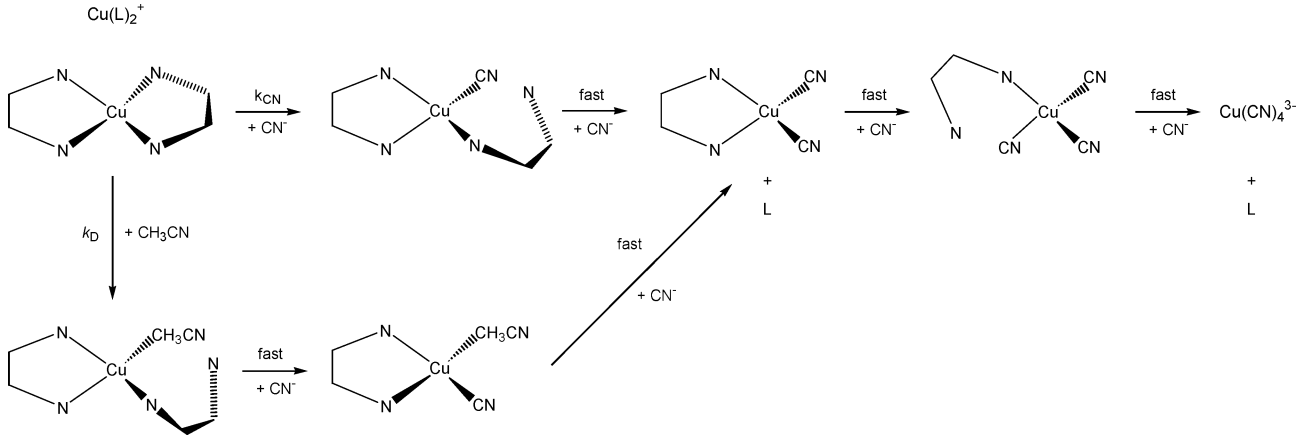

Figure 6. Schematic representation of the cyanide-assisted dissociation of the cuprous core of all the Cu(I) complexes examined in this work.

Table 5. Kinetic Parameters for the Decomplexation of **Cu(dmp)$_2$** and **Cu(dap)$_2$** by Cyanide

	Cu(dmp)$_2$		**Cu(dap)$_2$**	
	k_D (s^{-1})	k_{CN} (M^{-1} s^{-1})	k_D (s^{-1})	k_{CN} (M^{-1} s^{-1})
$CH_3CN/H_2O = 90/10$[a]	4.8 ± 0.6	820 ± 43	0.48 ± 0.01	6.5 ± 0.7
$CH_3CN/CH_2Cl_2/H_2O = 80/15/5$ (v/v/v)[b]	2.9 ± 0.3	1920 ± 20	0.50 ± 0.01	8.8 ± 0.4
$CH_3CN/CH_2Cl_2/H_2O = 48/50/2$ (v/v/v)[c]	0.53 ± 0.09	3421 ± 60	0.311 ± 0.003	14.9 ± 0.8

[a] $I = 0.1$ M (Bu_4NClO_4); $T = 25.0 \pm 0.1$ °C; ref 25. [b] $I = 0.1$ M ($Bu_4NCF_3SO_3$); $T = 25.0 \pm 0.1$ °C; ref 29. [c] $I = 0.05$ M (Bu_4NBF_4); $T = 25.0 \pm 0.2$ °C; uncertainties are estimated as 1σ.

For **Cu(L^n)$_2$**, the Student[32] test indicated that k_D was not statistically significant at the 95% probability level, and thus, the experimental data were adjusted to a line passing through the origin by linear regression.

In the presence of cyanide, the studied phenanthroline-based Cu(I) complexes dissociate according to a single rate-determining step mechanism. The experimental rate law (eq 2) supports a process which involves a dissociation path related to the intrinsic properties of the complex in the absence of cyanide, k_D, and a bimolecular cyanide-mediated pathway, k_{CN}. The first-order rate constant, k_D, then primarily reflects the thermodynamic stability of the complexes, whereas the bimolecular rate constant, k_{CN}, expresses the accessibility of the copper(I) center, giving information about the topography and the compactness around the metal ion.[17,25−27] Our data could agree very well with the following mechanism (Figure 6), which was already proposed for **Cu(dmp)$_2$** and **Cu(dap)$_2$**[25−27] and remains valid for the analogous complex **Cu(L^0)$_2$**, as well as for the four higher generations of dendrimers.

For the sake of comparison with the **Cu(L^n)$_2$** complexes, we have reexamined the bis(chelate) copper(I) complexes **Cu(dmp)$_2$** and **Cu(dap)$_2$**[17,25] under the experimental conditions of this work. Both have been studied previously under slightly different experimental conditions, and our results are consistent with former data. The corresponding k_D and k_{CN} values are collected in Table 5.

Due to intramolecular $\pi-\pi$ stacking interactions between the anisyl substituents and the phenanthroline core, **Cu(dap)$_2$** shows an entwined and stabilized structure[24] in which the Cu(I) center is noticeably more protected against the surrounding solvent than it is in **Cu(dmp)$_2$**. As it was already discussed,[17] the smaller k_D values for **Cu(dap)$_2$** reflect its higher thermodynamic stability when compared to the case of **Cu(dmp)$_2$**. The entwined structure of **Cu(dap)$_2$** is also more resistant to changes in solvent permittivity and viscosity (Table 5). For **Cu(L^n)$_2$**, the pathway related to the solvent-induced dissociation is disfavored and becomes insignificant with respect to the cyanide-assisted path. This suggests that the thermodynamic stability of the **Cu(L^n)$_2$** complexes is even higher than that of **Cu(dap)$_2$**. This may be related to the combination of a poorly distorted coordination geometry of the metallic core with effective interligand $\pi-\pi$ stacking interactions providing very good protection of the metal center from external contacts with the solvents. In the case of **Cu(dap)$_2$**, even if the $\pi-\pi$ interactions stabilize the complex, they are also responsible for the flattening distortion of the pseudotetrahedral geometry, facilitating contacts of the Cu(I) core with the solvents and thus allowing the solvent-induced dissociation.

Very interestingly, the bimolecular rate constant, k_{CN}, mainly reflects the shielding effect of the cuprous cation resulting from the bulkiness of the substituents directly connected to the 2,9-positions of the phenanthroline moieties. k_{CN} is indeed about 2 orders of magnitude lower for **Cu(dap)$_2$** than for **Cu(dmp)$_2$** and only 1 order of magnitude lower for **Cu(L^0)$_2$** than for **Cu(dmp)$_2$** (Tables 4 and 5). These data are in line with the degree of stacking shown by the respective X-ray structures (Figure 2) of these three bis-(chelate) Cu(I) complexes.[23,33]

The influence of the increased size of the polybenzyloxy substituents on the protection of the central Cu(I) bis-

(32) Commissariat à l'Energie Atomique. *Statistique Appliquée à l'Exploitation des Mesures*; Masson: Paris, 1979.

(33) The Cambridge Structural Database reference codes for the crystal structures of **Cu(dmp)$_2$** are CABKEV, DAWKOB, DMPNCU, DMPNCU01, DMPRCU, MPHCUN, and MPHCUN01.

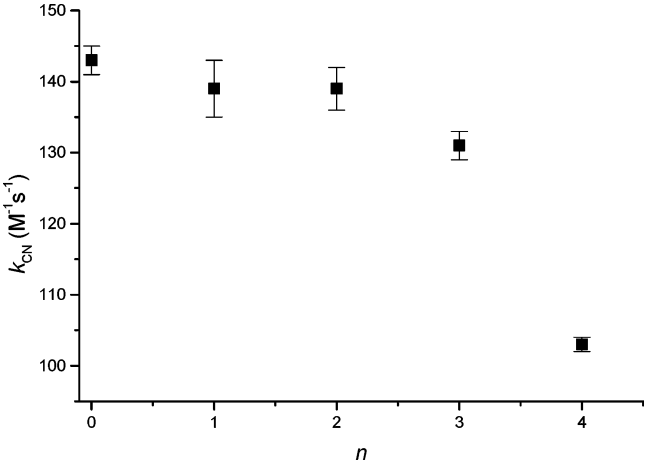

Figure 7. k_{CN} vs generation number (n) of the $\mathbf{Cu(L^n)_2}$ dendrimers. Solvent: $CH_2Cl_2/CH_3CN/H_2O$ = 50/48/2 (v/v/v); I = 0.05 M (Bu_4NBF_4); T = 25.0 ± 0.2 °C.

(phenanthroline) core was evaluated by comparing the results obtained within the series of $\mathbf{Cu(L^n)_2}$ complexes, with n = 0−4 (Scheme 1). It may be expected that, as the molecular size of the dendritic branches increases, their ability to encapsulate functional cores becomes more efficient and specific-site-isolated microenvironments may be created.[5,34] Both the dendritic shell and the microenvironment formed inside could then affect CN^- in its approach to the central core. When the size and bulkiness of the substituents attached to the Cu(I) bis(phenantroline) core are increased, a decrease of the bimolecular rate constants, k_{CN}, is observed (Table 4). Although the rate of the reaction of cyanide with the dendritic complexes slightly decreases from $\mathbf{Cu(L^0)_2}$ to $\mathbf{Cu(L^3)_2}$, a plot of k_{CN} versus generation number (n) (Figure 7) shows a noticeable discontinuity upon going from the third to the fourth generation, $\mathbf{Cu(L^3)_2} \Rightarrow \mathbf{Cu(L^4)_2}$. Since the cyanide anion is small (bond length ∼1.2 Å) and possesses a linear structure, the increasing bulkiness of the branches along the series of dendrimers up to $\mathbf{Cu(L^3)_2}$ does not comprise a big steric hindrance for it. The corresponding bimolecular rate constants indeed do not decrease drastically (Figure 7). A key problem seems to be the spatial structure and the location of the end groups. Flexible benzyloxy dendrons probably extend to the periphery of the molecule, and the central core remains open and accessible to CN^- to the same extent. The discontinuity in k_{CN} observed in the transition from the third to the fourth generation presumably corresponds to the process in which the branches fold back into the interior of the molecule. The conformation of the extended structure to the globular one in consequence gives rise to geometric encapsulation of the central Cu(I) bis(phenanthroline) complex and to the formation of a "lipophilic sphere" with a specific isolated interior. While approaching the central copper(I) core, CN^- experiences a more lipophilic environment which would affect its solvation.

Our data correlate well with previous studies reporting on the microenvironment created within Fréchet type dendritic branches[35] in which analysis of UV−vis absorption spectra of polyether branches with a *p*-nitroaniline solvatochromic probe attached to their focal point showed a pronounced batochromic shift of the absorption maxima in nonpolar solvents such as CCl_4 as well as in dichloromethane. The most dramatic change occurred between the third and the fourth generations. The same pattern of discontinuities was also evidenced in an earlier study on the same polyether dendrimers dealing with variation of the intrinsic viscosity with the generation number.[36] These changes are in line with computational studies, which led to the conclusion that higher generation dendrimers with flexible units had the highest density distribution at the center of the molecule.[37−40]

Conclusion

The copper(I) bis(chelate) complex $\mathbf{Cu(L^0)_2}$ has been prepared from 2,9-diphenethyl-1,10-phenanthroline and $Cu(CH_3CN)_4BF_4$. Interestingly, owing to the presence of the ethylene linker, the interligand $\pi-\pi$ stacking interactions between the phenyl rings and the phenanthroline subunits in $\mathbf{Cu(L^0)_2}$ do not induce significant distortions of the pseudotetrahedral symmetry around the Cu(I) center in the solid state or in solution. The latter observations are in sharp contrast with the strong distortion of the Cu(I) complexes of phenanthroline ligands with phenyl substituents directly attached on their 2,9-positions. Importantly, the combination of a poorly distorted coordination geometry of the metallic core with effective interligand $\pi-\pi$ stacking interactions provides very good protection of the metal center and the thermodynamic stability of $\mathbf{Cu(L^0)_2}$ is higher than that of the Cu(I) complexes of 2,9-diphenyl-1,10-phenanthroline ligands. Following the synthesis of $\mathbf{Cu(L^0)_2}$, dendrimers $\mathbf{Cu(L^{1-4})_2}$ with a Cu(I) bis(2,9-diphenethyl-1,10-phenanthroline) core surrounded by Fréchet type dendritic branches have been prepared. It is important to stress that the increased size of the surrounding dendritic wedges has no significant influence on the coordination geometry of the Cu(I) center. Therefore, the variations observed in the kinetics of the cyanide-assisted demetalation of dendrimers $\mathbf{Cu(L^n)_2}$ (n = 0−4) only reflect changes resulting from the presence of the dendritic branches. Actually, the discontinuity which has been observed between the third and the fourth generation could be explained by changes in the lipophilicity around the metallic core as a result of dendritic encapsulation. The cyanide-mediated dissociation of Cu(I) bis(phenanthroline) complexes is effectively sensitive to polarity. In conclusion, kinetic studies have provided interesting information not only on the accessibility of the central Cu(I) cation but also on other dendritic effects such as changes in micropolarity around the Cu(I) bis(phenanthroline) core.

(34) Dykes, G. M. *J. Chem. Technol. Biotechnol.* **2001**, *76*, 903.
(35) Hawker, C. J.; Karen, L. W.; Fréchet, J. M. J. *J. Am. Chem. Soc.* **1993**, *115*, 4375.
(36) Mourey, T. H.; Turner, S. R.; Rubenstein, M.; Fréchet, J. M. J.; Hawker, C. J.; Karen, L. W. *Macromolecules* **1992**, *25*, 2401.
(37) Karatasos, K.; Adolf, D. B.; Davies, G. R. *J. Chem. Phys.* **2001**, *115*, 5310.
(38) Murat, M.; Grest, G. S. *Macromolecules* **1996**, *29*, 1278.
(39) Boris, D.; Rubinstein, M. *Macromolecules* **1996**, *29*, 7251.
(40) Lescanec, R. L.; Muthukumar, M. *Macromolecules* **1990**, *23*, 2280.

Experimental Section

General Methods. Reagents and solvents were purchased as reagent grade and used without further purification. All reactions were performed in standard glassware under an inert Ar atmosphere. Evaporation and concentration were done at water aspirator pressure, and drying was done *in vacuo* at 10^{-2} Torr. Column chromatography: silica gel 60 (230−400 mesh, 0.040−0.063 mm) was purchased from E. Merck. Thin-layer chromatography (TLC) was performed on glass sheets coated with silica gel 60 F_{254} purchased from E. Merck; visualization was achieved by UV light. NMR spectra were recorded on a Bruker AC 200 spectrometer (200 MHz) with solvent peaks as reference. Mass measurements were carried out on a Bruker BIFLEX matrix-assisted laser desorption time-of-flight mass spectrometer (MALDI-TOF) equipped with SCOUT high resolution optics, an *X*−*Y* multisample probe, and a gridless reflector. Ionization was accomplished with the 337 nm beam from a nitrogen laser with a repetition rate of 3 Hz. All data were acquired at a maximum accelerating potential of 20 kV in the linear positive ion mode. The output signal from the detector was digitized at a sampling rate of 1 GHz. A saturated solution of 1,8,9-trihydroxyanthracene (dithranol Aldrich EC: 214-538-0) in CH_2Cl_2 was used as a matrix. Typically, a 1/1 mixture of the sample solution in CH_2Cl_2 was mixed with the matrix solution and 0.5 μL of the resulting mixture was deposited on the probe tip. Calibration was performed in the external mode with insulin (5734.6 Da) and ACTH (2465.2 Da). Elemental analyses were performed by the analytical service at the Institut Charles Sadron (Strasbourg, France).

Ligand L^0. A 2 M solution of LDA in THF (9.6 mL, 19.2 mmol) was added slowly to a solution of neocuproine (2.00 g, 9.6 mmol) in anhydrous THF (80 mL) at −78 °C under Ar. After 3 h, a solution of benzyl bromide (2.3 mL, 19.2 mmol) in THF (10 mL) was added dropwise. The resulting mixture was stirred for 2 h at −78 °C and then for 15 h at room temperature. The solution was then poured into ice water (150 mL). The mixture was extracted with CH_2Cl_2 (3 × 100 mL), and the combined organic layers were dried ($MgSO_4$), filtered, and evaporated. Column chromatography (SiO_2, CH_2Cl_2/2% MeOH) yielded **L^0** (2.05 g, 55%, colorless glassy product). ^{1}H NMR ($CDCl_3$, 200 MHz): 3.35 (m, 4H), 3.60 (m, 4H), 7.35 (m, 10H), 7.50 (d, J = 8 Hz, 2H), 7.73 (s, 2H), 8.15 (d, J = 8 Hz, 2H). ^{13}C NMR ($CDCl_3$, 50 MHz): 35.5, 40.9, 122.6, 125.5, 125.8, 127.2, 128.3, 128.5, 136.2, 141.8, 145.5, 161.9. Anal. Calcd for $C_{28}H_{24}N_2$: C, 86.56; H, 6.23; N, 7.21. Found: C, 86.47; H, 6.51; N, 7.11.

Compound 1. A 2 M solution of LDA in THF (9.2 mL, 18.4 mmol) was added slowly to a solution of neocuproine (1.90 g, 9 mmol) in anhydrous THF (60 mL) at −78 °C under Ar. After 3 h, a solution of *p*-[(*tert*-butyldimethylsilyl)oxy]benzyl bromide (6.10 g, 20 mmol) in THF (10 mL) was added dropwise. The resulting mixture was stirred for 2 h at −78 °C and then for 15 h at room temperature. The solution was then poured into ice water (150 mL). The mixture was extracted with CH_2Cl_2 (3 × 100 mL), and the combined organic layers were dried ($MgSO_4$), filtered, and evaporated. Column chromatography (SiO_2, CH_2Cl_2/2% MeOH) yielded **1** (2.30 g, 38%, colorless glassy product). ^{1}H NMR ($CDCl_3$, 200 MHz): 0.20 (s, 12H), 0.99 (s, 18H), 3.25 (m, 4H), 3.52 (m, 4H), 6.78 (d, J = 8 Hz, 4H), 7.19 (d, J = 8 Hz, 4H), 7.45 (d, J = 8 Hz, 2H), 7.72 (s, 2H), 8.13 (d, J = 8 Hz, 2H). ^{13}C NMR ($CDCl_3$, 50 MHz): 17.9, 25.5, 34.6, 41.0, 119.7, 122.5, 125.3, 126.9, 129.2, 134.3, 135.9, 145.3, 153.5, 161.7. Anal. Calcd for $C_{40}H_{52}O_2Si_2N_2$: C, 74.03; H, 8.08; N, 4.32. Found: C, 73.76; H, 8.17; N, 4.20.

Compound 2. A 1 M solution of TBAF in THF (2.6 mL, 2.6 mmol) was added slowly to a solution of **1** (0.60 g, 1 mmol) in THF (20 mL) at 0 °C. The resulting solution was stirred for 1 h at 0 °C. A few drops of water were then added, and the mixture was evaporated to dryness. Column chromatography (SiO_2, acetone/CH_2Cl_2 = 3/2) yielded **2** (0.41 g, 97%, colorless solid). ^{1}H NMR (acetone-d_6, 200 MHz): 3.04 (m, 4H), 3.31 (m, 4H), 6.75 (d, J = 8 Hz, 4H), 7.03 (d, J = 8 Hz, 4H), 7.55 (d, J = 8 Hz, 2H), 7.84 (s, 2H), 8.27 (d, J = 8 Hz, 2H), 8.67 (s, 2H).

General Procedure for the Preparation of Ligands L$^{1-4}$. A mixture of **2** (1 equiv), the appropriate benzylic bromide (2 equiv), K_2CO_3 (5 equiv), and 18-crown-6 (0.5 equiv) in acetone was refluxed for 48 h. The resulting mixture was diluted with CH_2Cl_2, filtered, and evaporated. The crude product was then purified, as outlined in the following text.

Ligand L^1. L^1 was prepared from benzyl bromide **G^{1}Br** and purified by column chromatography (SiO_2, CH_2Cl_2) (76%, colorless glassy product). ^{1}H NMR ($CDCl_3$, 200 MHz): 3.25 (m, 4H), 3.50 (m, 4H), 5.04 (s, 4H), 6.92 (d, J = 8 Hz, 4H), 7.25 (d, J = 8 Hz, 4H), 7.26−7.45 (m, 10H), 7.47 (d, J = 8 Hz, 2H), 7.72 (s, 2H), 8.13 (d, J = 8 Hz, 2H). ^{13}C NMR ($CDCl_3$, 50 MHz): 34.7, 41.2, 70.0, 114.7, 122.7, 125.6, 127.2, 127.4, 127.8, 128.5, 129.5, 134.2, 136.2, 137.2, 145.4, 157.0, 162.0. Anal. Calcd for $C_{42}H_{36}N_2O_2\cdot H_2O$: C, 81.52; H, 6.19; N, 4.53. Found: C, 81.57; H, 6.38; N, 4.23.

Ligand L^2. L^2 was prepared from **G^{2}Br** and purified by column chromatography (SiO_2, CH_2Cl_2) (96%, colorless glassy product). ^{1}H NMR ($CDCl_3$, 200 MHz): 3.27 (m, 4H), 3.53 (m, 4H), 4.98 (s, 4H), 5.04 (s, 8 H), 6.56 (t, J = 2 Hz, 2H), 6.64 (d, J = 2 Hz, 4H), 6.91 (d, J = 8 Hz, 4H), 7.26 (d, J = 8 Hz, 4H), 7.41 (m, 20H), 7.47 (d, J = 8 Hz, 2H), 7.72 (s, 2H), 8.13 (d, J = 8 Hz, 2H). Anal. Calcd for $C_{70}H_{60}O_6N_2$: C, 82.00; H, 5.90; N, 2.73. Found: C, 81.88; H, 5.96; N, 2.70.

Ligand L^3. L^3 was prepared from **G^{3}Br** and purified by column chromatography (SiO_2, CH_2Cl_2) (91%, colorless glassy product). ^{1}H NMR (CD_2Cl_2, 200 MHz): 3.25 (m, 4H), 3.49 (m, 4H), 4.97 (s, 12H), 5.02 (s, 16H), 6.55 (m, 6H), 6.68 (m, 12H), 6.91 (d, J = 8 Hz, 4H), 7.25 (d, J = 8 Hz, 4H), 7.27−7.43 (m, 40H), 7.45 (d, J = 8 Hz, 2H), 7.71 (s, 2H), 8.13 (d, J = 8 Hz, 2H). Anal. Calcd for $C_{126}H_{108}N_2O_{14}\cdot H_2O$: C, 79.97; H, 5.86; N, 1.48; O, 12.69. Found: C, 79.95; H, 5.93; N, 1.39; O, 12.37.

Ligand L^4. L^4 was prepared from **G^{4}Br** and purified by column chromatography (SiO_2, CH_2Cl_2) (99%, colorless glassy product). ^{1}H NMR (CD_2Cl_2, 200 MHz): 3.22 (m, 4H), 3.50 (m, 4H), 4.97 (m, 60H), 6.56 (m, 14H), 6.67 (m, 28H), 6.88 (d, J = 8 Hz, 4H), 7.22 (d, J = 8 Hz, 4H), 7.27−7.38 (m, 82H), 7.68 (s, 2H), 8.08 (d, J = 8 Hz, 2H). ^{13}C NMR ($CDCl_3$, 50 MHz): 29.6, 34.7, 41.1, 70.0, 101.5, 106.3, 114.7, 122.7, 125.6, 127.2, 127.5, 127.9, 128.5, 129.5, 134.2, 136.1, 136.7, 139.1, 139.7, 156.9, 160.0, 162.0. Anal. Calcd for $C_{238}H_{204}O_{30}N_2\cdot H_2O$: C, 79.61; H, 5.79; O, 13.82; N, 0.81. Found: C, 79.37; H, 5.88; O, 13.55; N, 0.81.

General Procedure for the Preparation of the Cu(I) Complexes Cu(L$^{0-4}$)$_2$. A solution of $Cu(CH_3CN)_4\cdot BF_4$ (1 equiv) in CH_3CN was added under an argon atmosphere at room temperature to a stirred, degassed solution of the appropriate ligand (2 equiv) in CH_2Cl_2. The solution turned orange-red instantaneously, indicating the formation of the complex. After 1 h, the solvents were evaporated and the crude product purified, as outlined in the following text.

Complex Cu(L^0)$_2$. Cu(L^0)$_2$ was prepared from **L^0** and purified by column chromatography (SiO_2, CH_2Cl_2/2% MeOH) (96%, red-orange crystals). ^{1}H NMR ($CDCl_3$, 200 MHz): 2.67 (m, 8H), 3.05 (m, 8H), 6.20 (d, J = 8 Hz, 8H), 6.93 (m, 12H), 7.80 (d, J = 8 Hz, 4H), 8.12 (s, 4H), 8.60 (d, J = 8 Hz, 4H). ^{13}C NMR ($CDCl_3$, 50 MHz): 35.3, 42.0, 125.2, 126.2, 126.5, 127.2, 127.9, 128.2, 139.2,

143.1, 160.4. Anal. Calcd for $C_{56}H_{48}N_4CuBF_4$: C, 72.53; H, 5.22; N, 6.04. Found: C, 72.72; H, 5.34; N, 6.05.

Complex Cu(L^1)$_2$. Cu(L^1)$_2$ was prepared from **L^1** and purified by column chromatography (SiO_2, CH_2Cl_2/2% MeOH) (95%, orange glassy product). ^{1}H NMR ($CDCl_3$, 200 MHz): 2.58 (m, 8H), 2.99 (m, 8H), 4.91 (s, 8H), 6.09 (d, J = 8 Hz, 8H), 6.44 (d, J = 8 Hz, 8H), 7.39 (m, 20H), 7.75 (d, J = 8 Hz, 4H), 8.02 (s, 4H), 8.52 (d, J = 8 Hz, 4H). ^{13}C NMR ($CDCl_3$, 50 MHz): 34.5, 42.3, 69.8, 114.5, 125.5, 126.4, 127.4, 129.9, 128.1, 128.24, 128.5, 131.5, 136.9, 137.8, 143.1, 157.0, 160.5. Anal. Calcd for $C_{84}H_{72}O_4N_4CuBF_4$: C, 74.64; H, 5.37; N, 4.15. Found: C, 74.36; H, 5.56; N, 3.62.

Complex Cu(L^2)$_2$. Cu(L^2)$_2$ was prepared from **L^2** and purified by column chromatography (SiO_2, CH_2Cl_2/2% MeOH) (72%, orange glassy product). ^{1}H NMR ($CDCl_3$, 200 MHz): 2.57 (m, 8H), 2.98 (m, 8H), 4.85 (s, 8H), 5.05 (s, 16H), 6.08 (d, J = 8 Hz, 8H), 6.42 (d, J = 8 Hz, 8H), 6.59 (t, J = 2 Hz, 4H), 6.65 (d, J = 2 Hz, 8H), 7.41 (m, 40H), 7.73 (d, J = 8 Hz, 4H), 8.00 (s, 4H), 8.49 (d, J = 8 Hz, 4H). ^{13}C NMR ($CDCl_3$, 50 MHz): 34.4, 42.2, 69.6, 70.0, 101.2, 105.6, 106.2, 114.5, 139.4, 143.1, 156.9, 160.1, 160.4. MALDI-TOF MS: 2112.2 ($[M - BF_4]^+$ calcd for $C_{140}H_{120}O_{12}N_4$: 2111.8). Anal. Calcd for $C_{140}H_{120}O_{12}N_4CuBF_4$: C, 76.40; H, 5.50; N, 2.55. Found: C, 76.54; H, 5.54; N, 2.49.

Complex Cu(L^3)$_2$. Cu(L^3)$_2$ was prepared from **L^3** and purified by column chromatography (SiO_2, CH_2Cl_2/2% MeOH) (92%, orange glassy product). ^{1}H NMR (CD_2Cl_2, 200 MHz): 2.54 (m, 8H), 2.93 (m, 8H), 4.86 (s, 8H), 4.94 (s, 16H), 5.00 (s, 32H), 6.04 (d, J = 8 Hz, 8H), 6.40 (d, J = 8 Hz, 8H), 6.56 (m, 12H), 6.67 (m, 24H), 7.29 (m, 80H), 7.68 (d, J = 8 Hz, 4H), 7.97 (s, 4H), 8.46 (d, J = 8 Hz, 4H). MALDI-TOF MS: 3809.7 ($[M - BF_4]^+$ calcd for $C_{252}H_{216}N_4O_{28}Cu$: 3808.5). Anal. Calcd for $C_{252}H_{216}N_4O_{28}CuBF_4 \cdot H_2O$: C, 77.27; H, 5.61; N, 1.43. Found: C, 77.09; H, 5.46; N, 1.25.

Complex Cu(L^4)$_2$. Cu(L^4)$_2$ was prepared from **L^4** and purified by column chromatography (SiO_2, CH_2Cl_2/2% MeOH) (85%, orange glassy product). ^{1}H NMR ($CDCl_3$, 200 MHz): 2.49 (m, 8H), 2.89 (m, 8H), 4.77 (s, 8H), 4.93 (m, 48H), 4.97 (m, 64H), 5.99 (d, J = 8 Hz, 8H), 6.37 (d, J = 8 Hz, 8H), 6.53 (m, 84H), 7.29 (m, 160H), 7.59 (d, J = 8 Hz, 4H), 7.90 (s, 4H), 8.37 (d, J = 8 Hz, 4H). MALDI-TOF MS: 7203.6 ($[M - BF_4]^+$ calcd for $C_{476}H_{408}N_4O_{60}$: 7201.8). Anal. Calcd for $C_{476}H_{408}N_4O_{60}CuBF_4 \cdot CH_2Cl_2$: C, 77.63; H, 5.60; N, 0.76. Found: C, 77.72; H, 5.64; N, 0.57.

X-ray Crystal Structure of Cu(L^0)$_2$. The red-orange crystal used for the diffraction study was produced by slow diffusion of MeOH into a CH_2Cl_2 solution of **Cu(L^0)$_2$** ($C_{112}H_{96}N_8Cu_2B_2F_8$, M_r = 1854.76): Triclinic space group $P\bar{1}$, Z = 2, a = 13.9285(3) Å, b = 17.4020(4) Å, c = 19.2839(5) Å, α = 83.339(5)°, β = 87.924(5)°, γ = 87.230(5)°, V = 4634.9(2) Å^3. The parameters for the data collection and refinement of diffraction data as well as the atomic coordinates and the thermal parameters are contained in the Supporting Information.

UV−Visible Spectrophotometry. The spectrophotometric studies were carried out on a Kontron Uvikon 941 spectrophotometer equipped with 1 cm quartz cells (Hellma) thermostated at 25.0 ± 0.2 °C. Absorbance data were recorded in a range of wavelengths from 250 to 650 nm.

Kinetic Studies. All the experiments were carried out in a freshly prepared homogeneous ternary solvent, $CH_2Cl_2/CH_3CN/H_2O$ = 50/48/2 (v/v/v). The ionic strength was adjusted to 0.05 M with tetrabutylammonium tetrafluoroborate (Aldrich, 99%). The scavenger reagent tetraethylammonium cyanide (Fluka, purum) was always used in large excess with respect to the concentrations of the Cu(I) complexes ($\sim 1.5 \times 10^{-5}$ M) in order to obtain pseudo-first-order conditions. The cyanide concentrations were varied in a range from $\sim 6 \times 10^{-4}$ to $\sim 2.4 \times 10^{-3}$ M.

CAUTION! Tetraethylammonium cyanide is highly toxic, and since hydrogen cyanide is being generated in the presence of acid, gloves and a fume hood should be used when handling this compound.[41] Sodium hypochlorite was used in order to oxidize and destroy cyanide anions in solution.[42]

The kinetic studies were performed at a fixed wavelength corresponding to the absorption maximum of the MLCT band of the bis(phenanthroline) Cu(I) complex under study using a stopped-flow spectrophotometer (Applied Photophysics SX-18MV). The reactants were mixed in a 1 cm optical cell, and the temperature was maintained constant at 25.0 ± 0.2 °C. The data sets, averaged out of at least three replicates, were recorded and analyzed with the commercial software Biokine.[43] This program fits up to three exponential functions to the experimental curves with the Simplex algorithm[44] after initialization with the Padé−Laplace method.[45,46]

Acknowledgment. This research was supported by the CNRS and the French Ministry of Research (ACI Jeunes Chercheurs to J.-F.N.). E.G.-K. thanks the CNRS and Y.R. the Direction de la Recherche of the French Ministry of Research for their fellowships. We further thank Dr. D. Felder for the initial preparation of **Cu(L^0)$_2$**, L. Oswald for technical help, M. Schmitt for high field NMR spectra, and J.-M. Strub for MS measurements. The authors are grateful to Dr. C. O. Dietrich-Buchecker for samples of **Cu(dmp)$_2$** and **Cu(dap)$_2$**.

Note Added after ASAP: Some errors appeared in the identification of the contributing institutions in the version of this paper posted ASAP on April 2, 2004. The institutions are correctly identified in the version posted on April 16, 2004.

Supporting Information Available: Six figures showing electronic spectra of **Cu(L^1)$_2$**, **Cu(L^2)$_2$**, and **Cu(L^3)$_2$**; plots of the pseudo-first-order rate constant, k_{obs}, as a function of cyanide concentration for **Cu(dmp)$_2$**, **Cu(dap)$_2$**, **Cu(L^0)$_2$**, **Cu(L^1)$_2$**, **Cu(L^2)$_2$**, and **Cu(L^3)$_2$**; an ORTEP drawing of **Cu(L^0)$_2$**; and ^{1}H NMR spectra of **Cu(L^1)$_2$**, **Cu(L^2)$_2$**, and **Cu(L^4)$_2$** and CIF files. This material is available free of charge via the Internet at http://pubs.acs.org.

IC049945Y

(41) Chemical Safety Data Sheet SD-67. Hydrocyanic acid; Manufacturing Chemists' Association: Washington, DC, 1961.
(42) Gerritsen, C. M.; Margerum, D. W. *Inorg. Chem.* **1990**, *29*, 2757.
(43) *Biokine*; Bio-Logic Company: Echirolles, France, 1991.
(44) Nelder, J. A.; Mead, R. *Comput. J.* **1965**, *7*, 308.
(45) *Enzfitter*; Leatherbarrow, J., Ed. Biosoft: Cambridge, U.K., 1987.
(46) Yeramian, E.; Claverie, P. *Nature* **1987**, *326*, 169.